ChemPubSoc Europe

DOI: 10.1002/open.201900150

Open Access ChemistryOPEN Full Paper

Ortho-Quinone Methide Driven Synthesis of New *O,N*- or *N,N*-Heterocycles

István Szatmári,*[a, b] Khadija Belasri,[a, b] Matthias Heydenreich,[c] Andreas Koch,[c] Erich Kleinpeter,*[c] and Ferenc Fülöp*[a, b]

To synthesize functionalized Mannich bases that can serve two different types of *ortho*-quinone methide (*o*-QM) intermediates, 2-naphthol and 6-hydroxyquinoline were reacted with salicylic aldehyde in the presence of morpholine. The Mannich bases that can form *o*-QM and *aza*-*o*-QM were also synthesized by mixing 2-naphthol, 2-nitrobenzaldehyde, and morpholine followed by reduction of the nitro group. The highly functionalized aminonaphthol derivatives were then tested in [4+2] cycloaddition with different cyclic imines. The reaction proved to be both regio- and diastereoselective. In all cases, only one reaction product was obtained. Detailed structural analyses of the new polyheterocycles as well as conformational studies including DFT modelling were performed. The relative stability of *o*-QMs/*aza*-*o*-QM were also calculated, and the regioselectivity of the reactions could be explained only when the cycloaddition started from aminodiol **4**. It was summarized that starting from diaminonaphthol **25**, the regioselectivity of the reaction is driven by the higher nucleophilicity of the amino group compared with the hydroxy group. 12H-benzo[a]xanthen-12-one (**11**), formed via *o*-QM formation, was isolated as a side product. The proton NMR spectrum of **11** proved to be very unique from NMR point of view. The reason for the extreme low-field position of proton H-1 could be accounted for by theoretical calculation of structure and spatial magnetic properties of the compound in combination of ring current effects of the aromatic moieties and steric compression within the heavily hindered H(1)-C(1)-C(12b)-C(12a)-C(12)=O structural fragment.

1. Introduction

The Mannich reaction is one of the most important basic reaction types in organic chemistry for C–C and C–N bond formation.[1–3] The classical Mannich product arises from the condensation reaction of a compound containing at least one active hydrogen atom with formaldehyde and a secondary amine.[4] A special variation of this latter reaction when formaldehyde is replaced by benzaldehyde, the secondary amine by ammonia, and the C–H acid by an electron-rich aromatic compound such as 2-naphthol. The reaction was first developed by Mario Betti and the aminonaphthol synthesized in this way became as Betti base.[5] This modified three-component Mannich reaction (mMR) was then extended to apply 1-naphthol, quinolinol or isoquinolinol as electron-rich aromatic compounds.[5–6] Mechanistically, the bifunctional product is formed by the nucleophilic addition of the electron-rich aromatic compound on the C=N bond formed by in situ condensation of the aldehyde and amine. As a consequence of the two or more functional groups in the structures of the Mannich bases prepared via such modified reactions, one of the most important areas of application is the synthesis of new heterocycles.[5,7]

Another proposed mechanism for the synthesis of modified Mannich bases is via formation of an *ortho*-quinone methide (*o*-QMs) intermediate that is generated from the aldehyde and the electron-rich aromatic compound such as 2-naphthol. This intermediate reacts with the nucleophile to form the final Mannich products.[8] Accordingly, *o*-QMs can also be generated from the Mannich bases after thermal elimination of the amine. This reactive moiety can be stabilized by reacting with different dienophiles.[5,9,10] One of the possibilities is when the formed *o*-QMs reacts with electron-rich aromatic compounds. Accordingly, Rueping et al.[11] recently published reactions between aza-*o*-QMs generated in situ from α-substituted *ortho*-aminobenzyl alcohols and substituted indoles catalyzed by *N*-triflylphosphoramides (NTPAs). The process provided new C-2- and C-3-functionalized indole polyheterocycles in good yields with 90–99% ee.[11]

The preparation of novel condensed polyheterocycles is a relatively new area of the chemistry of *o*-QMs generated from Mannich bases. In this case, the [4+2] cycloaddition take place between the *o*-QMs and cyclic imines (containing C=N bond). Our research group developed for the first time the reaction of 1-aminoalkyl-2-naphthols with 3,4-dihydroisoquinoline as cyclic imine.[12] The reaction was then extended starting from 2-

[a] Dr. I. Szatmári, K. Belasri, Prof. Dr. F. Fülöp
Institute of Pharmaceutical Chemistry and MTA-SZTE Stereochemistry Research Group, University of Szeged, H-6720 Szeged, Eötvös u. 6, Hungary
E-mail: szatmari.istvan@pharm.u-szeged.hu
fulop@pharm.u-szeged.hu
[b] Dr. I. Szatmári, K. Belasri, Prof. Dr. F. Fülöp
Institute of Pharmaceutical Chemistry, University of Szeged, Interdisciplinary excellence center
[c] Dr. M. Heydenreich, Dr. A. Koch, Prof. Dr. E. Kleinpeter
Department of Chemistry, University of Potsdam, Karl-Liebknecht-Str 4-25, D-14476 Potsdam (Golm), Germany
E-mail: ekleinp@uni-potsdam.de

Supporting information for this article is available on the WWW under https://doi.org/10.1002/open.201900150

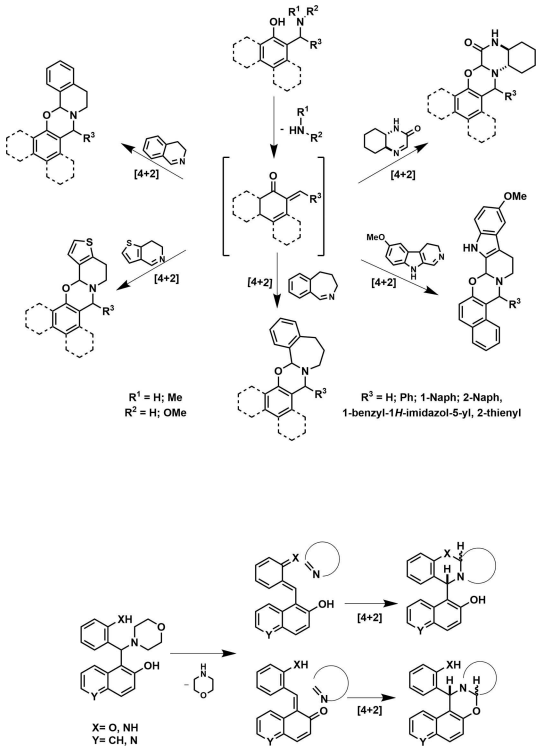

Figure 1. Summary of previous work and the results of this study.

aminoalkyl-1-naphthols and other C=N dienophiles (cyclic imines) preparing new naphthoxazino-isoquinoline, -benzazepine and -thienopyridine derivatives.[13] At the same time, Osyanin *et al.*[14] reported the same reaction extended by various substituted aminonaphthols achieving the syntheses in ethanol at 78 °C (Figure 1).

To the best of our knowledge, the transformation of bifunctional Mannich bases, which can serve two different types of *o*-QMs has not been investigated. According to this, our first aim was to synthesize new functionalized aminonaphthol derivatives. Our further aim was to study the scope and limitations of the applicability of these aminonaphthols in [4+2] cycloaddition. Furthermore, we wanted to investigate the influence of the relative stability of the formed *o*-QMs and/or the dienophile on the structure of the final product. Finally, both structure and conformational behavior of the novel polyheterocycles was studied by NMR spectroscopy and accompanying theoretical quantum chemical (QC) calculations.

2. Results and Discussion

2.1. Synthesis

First, the synthesis of the functionalized precursor aminonaphthol derivative was achieved. Accordingly, 2-naphthol and salicylic aldehyde were reacted in the presence of morpholine as a cyclic secondary amine. The reaction was carried out under neat conditions at 80 °C. The optimal reaction time was 5 hours. The progress of the synthesis was followed by TLC that showed the formation of two main products. The separation of the desired aminonaphthol from the side product was achieved based on the concept that the derivative we want to produce contains basic nitrogen. Therefore, the work-up procedure was optimized by adding dichloromethane to the mixture and then extracting with 2% hydrochloric acid. Then the aqueous phase was alkalized with sodium carbonate and extracted with dichloromethane. The collected organic layers were dried, evaporated, and crystallized to isolate the expected bifunctional compound **4** (Scheme 1).

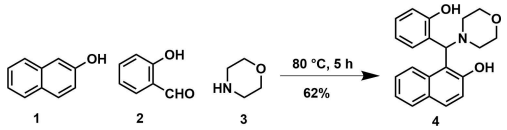

Scheme 1. The synthesis of the functionalized aminonaphthol **4**.

To test the behavior of this highly functionalized aminonaphthol **4** in [4+2] cycloaddition, it was first reacted with β-carboline **6**.[15] The reaction was performed in 1,4-dioxane by using 1.5 equivalents of the cyclic imine **6**. To accelerate the reaction, microwave irradiation was. applied instead of conventional heating due to its positive effects (shorter reaction, improved yields). Because of the thermal decomposition of starting material **4**, two types of *o*-QM intermediate (**5a** and **5b**) can be formed. The stabilization of these reactive moieties with the dienophile (3,4-dihydro-β-carboline) can lead to the formation of two regioisomeric products: benzoxazino-β-carboline **7** and naphthoxazino-β-carboline **8** (Scheme 2). Since

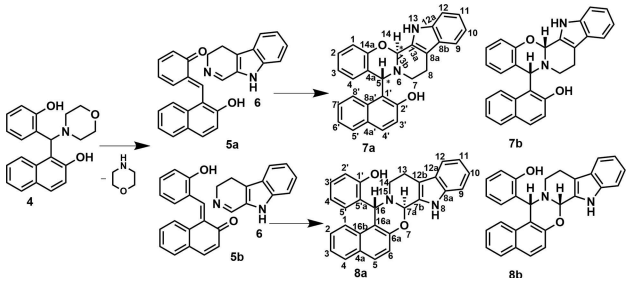

Scheme 2. [4+2] cycloaddition between **4** and 3,4-dihydro-β-carboline.

during the reaction two new stereogenic centers are generated, two regioisomers (**7** and **8**) and two epimeric structures (**a** and **b**) can be obtained.

The reaction was monitored by TLC, and the composition of the crude reaction mixture was verified by ^{1}H-NMR analysis. In our first experiment the reaction was performed at 60 °C. After a relatively short reaction time, the desired product was isolated in a yield of 47%; since the yield was not satisfactory, the reaction was repeated at 80 °C and 100 °C. Results are summarized in Table 1. 80 °C and 20 minutes reaction time was found to be the optimal reaction conditions. The detailed NMR spectroscopic and computational stereochemistry analysis (see

Table 1. Reaction Conditions for Preparation of Compounds **8a**, **14a**, **16a** and **22a**

Product	Time	Temperature (°C)	Yield (%)
8a	20 min	60	47
		80	*89*
		100	22
14a	20 min	60	55
		80	*87*
		100	27
17a	20 min	60	36
		80	*92*
		100	21
22a	20 min	60	24
	40 min	80	36
	60 min	*100*	*90*
	40 min	*120*	67

2.2.) proved that the formed regioisomer is a naphthoxazine and the relative configuration of C-7a and C-16 is *trans* (**8a**, Scheme 2). By using higher temperatures (*e.g.* 100 °C) the desired product was isolated with only a poor yield (22%), while the formation of a new spot in TLC was observed. After isolation, the side product was identified (see **2.3.**) to be 12*H*-benzo[*a*]xanthen-12-one **11**.[16] that was isolated in a yield of 37%. The xanthone derivatives are the core structure of many natural compounds and pharmaceuticals and, at the same time, they are versatile synthons to achieve new heterocycles. Most of the known methods for their synthesis either require rather complicated and/or expensive starting materials or involve multistep transformations by using different catalysts.[17–20] In our case the formation of **11** can be explained by the mechanism depicted in Scheme 3. Accordingly, the formed *o*-

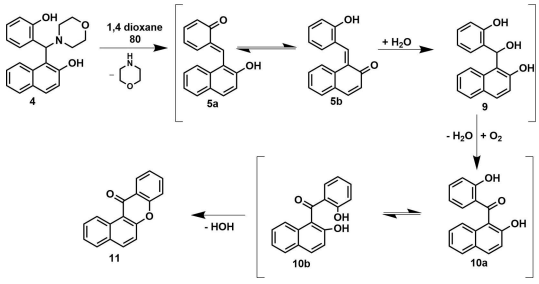

Scheme 3. Plausible mechanism for the formation of benzo[*a*]-xanthen-12-one

QMs (**5a** or **5b**) are stabilized by water addition to form triole **9**. The oxidation to dihydroxy keton **10a** followed by water elimination can led to the formation of **11**. It was proposed that both the basicity of the leaving morpholine and the presence of β-carboline are necessary for the formation of **11**. Therefore, the reaction was repeated starting from **4** by using Et_3N as a base in 1,4-dioxane at 100 °C. The reaction was performed under microwave irradiation, and the desired xanthone derivative **11** was obtained in a yield of 71%. This method is the first synthesis of **11** via *o*-QM intermediates **5a** and **5b** starting from a highly functionalized Mannich base **4**. The ^{1}H NMR spectrum of 12*H*-benzo[*a*]xanthen-12-one (**11**) is very interesting and will be discussed below (*see* **2.3.**).

The extension of the reaction was investigated by using other cyclic imines as starting compounds. Therefore, 3,4-dihydroisoquinoline[21] and 6,7-dihydrothieno[3,2-*c*]pyridine[22] were selected as representative cyclic imines (Scheme 4). The

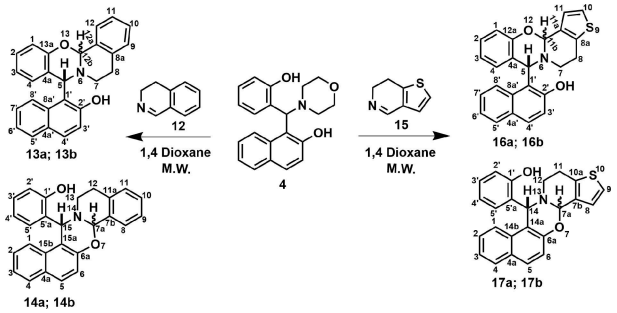

Scheme 4. Reaction of aminonaphthol **4** with cyclic imines.

reactions were performed at three different temperatures (60 °C, 80 °C, and 100 °C). The yields obtained are summarized in Table 1. It can be concluded that for these latter synthesis, the optimal reaction condition was 20 minutes at 80 °C. After isolation of the desired polyheterocycles (**14a** and **17a**), both the diastereo- and regioselectivity of the reaction were confirmed. In all cases, the NMR spectra of the crude products show the formation of single product.

Our original idea was that the formation of the products is influenced by the relative stability of the *o*-QM intermediates. Consequently, our next aim was to investigate how an additional heteroatom (nitrogen) will modify the relative stability of the formed *o*-QMs, and how it will influence the composition of the product mixture. The synthesis of bifunctional quinolinol **19** was achieved by reacting 6-hydroxyquinoline **18** as *N*-containing 2-naphthol analogue with salicylic aldehyde in the presence of morpholine. The desired product was isolated and purified by crystallization from *n*-hexane (see *Experimental Part*). The reactivity of **19** was tested in the [4+2] cycloaddition reaction with 3,4-dihydroisoquinoline as representative cyclic imine. After a reaction time of 60 min. at 100 °C, TLC did not show the presence of the starting materials. The reaction mixture was cooled and product **22a** was isolated by treatment with MeOH (Scheme 5). From the varied reaction temperature (60 °C, 80 °C, 100 °C), 100 °C was found to be the optimal one.

The composition of the crude reaction mixtures was also checked, and both the regio- and the diastereoselectivity of the reaction were confirmed by the formation of a single product. The detailed NMR analysis proved that the isolated compound is the *trans* isoquinolino[1′,2′:2,3][1,3]oxazino[5,6-*f*]quinolin (**22a**, see **2.2.**).

Our further aim was to synthesize diaminonaphthol, which can lead to two types of *o*-QMs during the cycloaddition reaction. Furthermore, in this case, one of them is an *aza*-*o*-QM, where a special relative stability can be predicted. Accordingly, 2-naphthol was reacted with morpholine in the presence of 2-

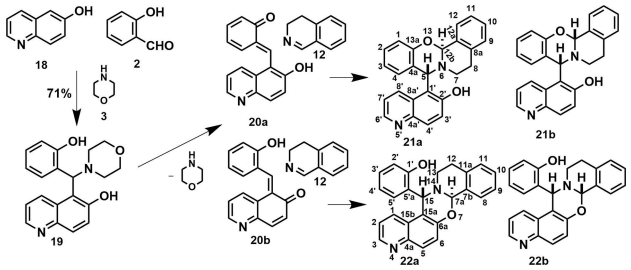

Scheme 5. Synthesis and transformation of aminoquinolinol **19**.

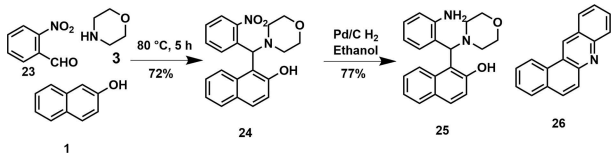

Scheme 6. The synthesis of the diaminonaphthol **25**.

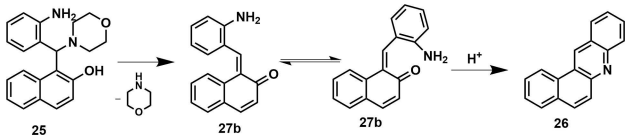

Scheme 7. Plausible mechanism for the formation of benz[a]acridine **26**.

nitrobenzaldehyde. After a reaction time of 5 hours at 80 °C, aminonaphtol derivative **24** was isolated (Scheme 6). The next step was the reduction of nitro compound **24** via hydrogenation in the presence of Pd/C. The desired diaminonaphthol **25** was isolated after 1 hour reaction time, by crystallization in a yield of 77 %. According to TLC, the reaction proved to be sensitive to the reaction time. After 1 hour, the formation of a side product was observed. When the reaction was repeated by using longer reaction time (5 hours), it led almost completely to the formation of the side product. The mixture was purified by column chromatography and the NMR and MS spectra together with the melting point proved that the isolated compound is benz[*a*]acridine (**26**).[23]

The possible reaction pathway to furnish **26** via formation of the *o*-QM intermediate **27** is depicted in Scheme 7. The synthesis of **26** has already been published starting from aniline and 1-*N*,*N*-dimethylaminomethyl-2-naphthol.[23] Accordingly, the *o*-QM mediated synthesis of **26** can be interpreted as a new synthetic method to prepare benz[*a*]acridine derivatives.

In our first experiment, bifunctional derivative **25** was reacted with β-carbolin as cyclic imine. The reaction was performed by applying three different temperatures, using microwave irradiation, leaving the previously applied solvent (1,4-dioxane) unchanged. Based on the crude product NMRs, the reaction again proved to be regio- and diastereoselective, and independently of the applied conditions (Table 2), quinazoline **28 b** was also isolated as a single product (Scheme 8). Note, that in this case the ring closure went to the direction of forming quinazoline, and the relative configuration of H-5 and

Table 2. Reaction Conditions for Preparation of Compounds **28 b, 30 b and 32 b**

Product	Time	Temperature (°C)	Yield (%)
28 b	20 min	60	40
		80	*91*
		100	20
30 b	20 min	60	40
		80	*89*
		100	19
32 b	20 min	60	36
		80	*92*
		100	21

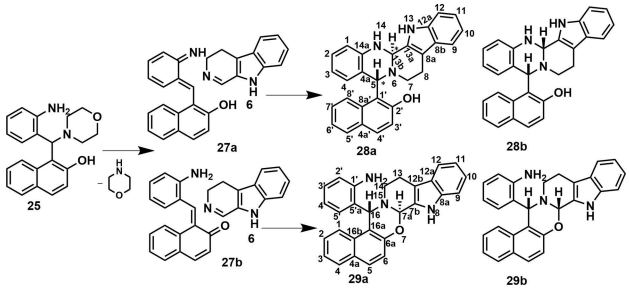

Scheme 8. [4 + 2] cycloaddition between **25** and 3,4-dihydro-β-carboline.

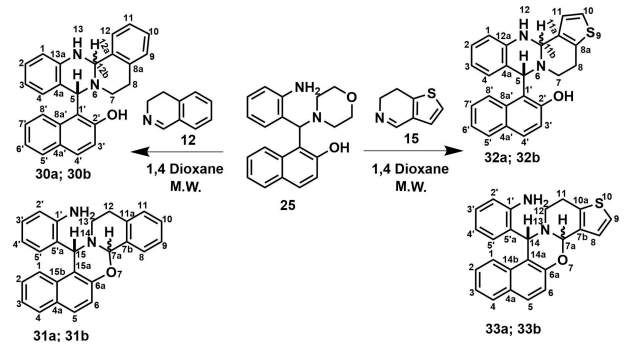

Scheme 9. Reaction of diaminonaphthol **25** with cyclic imines.

H-13b was found from the detailed NMR spectra to be cis, supported by the parallel DFT calculations (see **2.2.**).

The reaction was extended by testing 3,4-dihydroisoquinoline and 6,7-dihydrothieno[3,2-*c*]pyridine as cyclic imines (Scheme 9). After a reaction time of 20 min at 80 °C, the desired heterocycles were isolated in good yields as depicted in (Table 2). These optimal conditions were selected from three different temperatures listed in Table 2. In all cases, the regio- and diastereoselectivity of the reaction were proved by the crude product NMR spectra. The detailed NMR measurements adequately showed that the isolated products are the corresponding condensed quinazoline derivatives **30 b** and **32 b**.

As it was proved experimentally and supported by theoretical calculations, the regioselectivity of the [4 + 2] cycloaddition is influenced by the structure of the starting bifunctional compounds. Namely, starting from aminodiols (**4**), *trans*-naphthoxazines (**8 a, 14 a and 17 a**) were formed, while diaminonaphthol (**25**) led to the formation of *cis*-quinazolines (**28 b,**

30b, and **32b**). It was surmised that this undesired selectivity resulted from the relative stability of the *o*-QM intermediates. Therefore, the relative energy for the pair of *o*-QMs (**5a**, **5b**) and (**27a**, **27b**) were calculated.

In the case of o-QMs **5a** and **5b**, **5b** was found to have about 10 kcal/mol lower energy compared with **5a**. This finding is in complete agreement with our experimental result that the naphtholic hydroxyl group is participating in the cycloaddition reaction, *i.e.*, the reaction leads to the formation of the naphthoxazines.

Comparing the energy values calculated for **27a** and **27b**: *o*-QM **27b** was found to have lower energy (about 9 kcal/mol) than the *aza*-*o*-QM **27a**. This result cannot explain the fact that quinazolines were found experimentally to be the single products. It means that in this case the higher nucleophilicity of the amino group compared with naphtholic hydroxyl group overwrite the theory that only the relative stability of *o*-QMs is influencing the outcome of the cycloaddition reaction.

2.2. Structural and Conformational Analysis

The complete NMR of the educts shows different structures with different ring formations depending on the starting material **4**, with an OH group, or **25** with an NH_2 group at *ortho* position. All products starting from **4** showed the same regioselectivity and stereochemistry while those starting from **25** were found to have different regio- and stereoselectivity, but the same within the series. This will be shown by compounds **16a,b** or **17a,b** and **32a,b** or **33a,b**, selected as examples. For the corresponding structure elucidation, both the NMR spectra (chemical shift, coupling constants, NOE's) and quantum chemical calculations are examined.

To get the preferred regio- and stereoisomers of **16a,b** or **17a,b** and **32a,b** or **33a,b** the *trans/cis* diastereomers (RS/SR and RR/SS) of the regioisomers were calculated by the DFT method. Both the most stable structures and the corresponding energy differences are given in Figure 2; hereby, **17a** and **32b**, respectively, could be identified to be the most stable structures. Energy differences around 1 kcal / mol to the next coming structure are rather unequivocal. Consequently, structures of *trans*-isomer **17a** and of *cis*-isomer **32b** were compared with available experimental NMR [$\delta(^1H)$/ppm, $\delta(^{13}C)$/ppm, $^nJ_{H,H}$/Hz)] and spatial NMR information (NOEs).

First, all ^1H and ^{13}C NMR chemical shifts for **17** could be unequivocally assigned. Hereby, the OH-bearing positions 6a and 1′ are crucial, and the AX spin system of H-5 and H-6 protons can serve as useful starting point. It is the only spin system of aromatic protons with two doublets and the characteristic *ortho*-coupling constant of *ca.* 9 Hz.[7,24] The low-field doublet (at 7.72 ppm) was assigned to the H-5 proton. The long-range coupling constant of the H-5 proton to the ^{13}C signal of C-6a (at 151.0 ppm) unequivocally assigns this carbon atom and can serve as entry into the sequence of ^{13}C signals: Thus, the other OH-bearing carbon atom C-1′ must have the chemical shift of 156.7 ppm. Based on this entry, assignment of the other aromatic carbon atoms using direct and long-range connectivities can be easily realized.

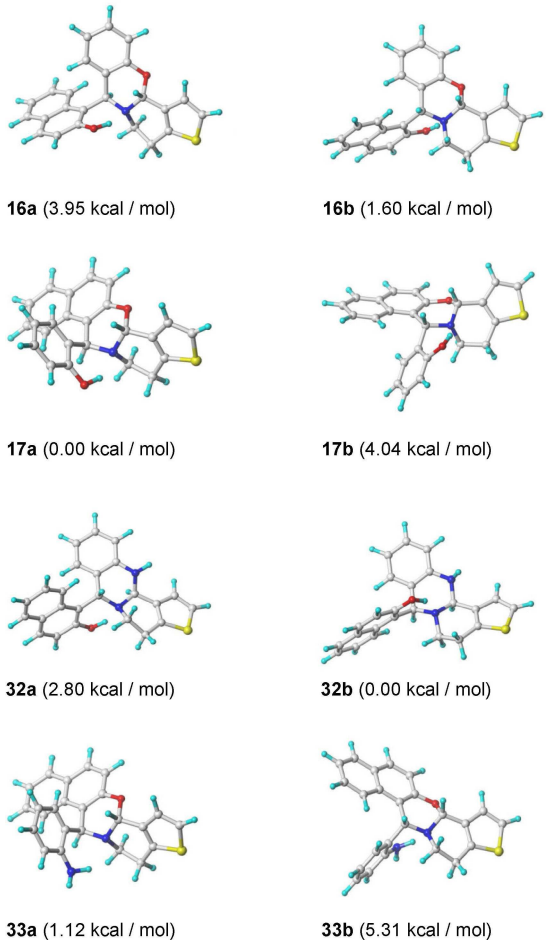

Figure 2. The most stable structures of the regioisomeric (**16** or **17**; **32** or **33**) heterocycles including their *trans* (**a**) and *cis* (**b**) diastereomeric possibilities.

Another ^1H NMR and the HMBC spectrum were recorded in [D_6]DMSO as solvent to stabilize the OH-group. Along the analysis, long-range connectivities between OH and the carbons at positions 1′, 2′, and 5′a, respectively, together with a medium NOE between H-7a and H-8 (2.85 Å from quantum chemical calculations) unambiguously lead to the regioisomer **17**. Some more representative long-range connectivities corroborate this structure: From H-14 to carbons C-1′, C-5′a, C-6a, C-14a, and C-14b; from H-5 to C-4, C-6a, and C-14b, and from H-8 to C-7a, C-7b and C-10a, respectively. In addition, the obtained NOE's agree only with the stereochemistry of **17a**: the protons H-7a and H-14 are in *trans* position. The corresponding NOE's do support this conclusion: strong NOE between H-1 and H-14 (2.17 Å), medium NOE between H-1 and H-5′ (3.14 Å) and the weak NOE between H-7a and H-11eq (4.52 Å), respectively (*cf.* Table 3).

Starting from aniline derivative **25**, instead of the phenol analogue **4**, another type of ring closure was observed. Again, for exemplary purposes, the stereochemical analysis is described for compound **32**. The two low-field ^{13}C NMR signals at 155.5 and 142.2 ppm, respectively, can be easily assigned to the

Table 3. Computed distances and measured NOE's for **32b**.

Positions	computed distances (Å)	NOE
H-11/H-12	2.81	Medium
H-11/H-11b	3.14	Medium
H-8ax/H-12	4.42	Weak
H-7eq/H-5	2.78	Medium
H-7ax/H-5	2.51	Strong
H-7eq/H-12	4.89	Weak
H-7ax/H-11b	2.54	Strong
H-5/H-4	2.97	Medium
H-5/H-12	4.28	Weak
H-5/H-11b	2.44	Strong
H-5/H-8′	1.92	Strong
H-4/H-8′	2.89	Medium
H-12/H-11b	2.91	Medium

two heteroatom bearing aromatic carbons: 155.5 ppm is assigned to the C-2′ signal due to the higher electronegativity of oxygen in comparison with nitrogen (C-12a: 142.2 ppm). This is corroborated by long-range connectivities between H-4′ and C-2′, and between H-5 and C-12a. A $^{3}J_{H\text{-}16b,H\text{-}12}$ coupling constant of 5.8 Hz and long-range connectivities of the OH proton to C-2′, C-3′ and C-4′ (weak), respectively, support only the presence of regioisomer **32**. A strong NOE between H-5 and H-11b (calculated distance: 2.44 Å) confirms additionally the *cis* configuration of H-5 and H-11b. Actually, **32b** proves to be the only possible configuration, where the calculated distances fit with the experimentally determined NOE's (see Table 3).

Interestingly, in both compounds a large difference in the ^{1}H NMR chemical shifts between H-1 and H-5′ (in **17a**) and between H-8′ and H-4 (in **32b**) was observed. These extremely large chemical shift differences of $\Delta\delta = 1.04$ ppm in the first and $\Delta\delta = 1.62$ ppm in the latter case correspond to their computed different distances of 3.14 Å and 2.89 Å, respectively. This points to strong steric compression within the corresponding fragments. In addition, the influence of ring current effects of the present aromatic moieties in **17a** and **32b** can be expected (see **2.4.**).

The same *trans* configuration as in **17a** was found in the stereochemically analogous β-carboline **8a** and isoquinoline derivatives **14a**, and the *cis* configuration as in **32b** was also found in the structurally analogous new *N,N*-heterocyclic compounds **30b** and **28b**, respectively.

2.3. ^{1}H and ^{13}C NMR Spectra of 12*H*-Benzo[*a*]xanthen-12-one (11)

The ^{13}C chemical shifts of the carbon atoms in 12*H*-benzo[*a*]xanthen-12-one (**11**)[25] (*cf.* Figure 3) were found as expected. That is, the aromatic *C*-H carbon atoms resonate in the common range for this kind of carbons ($\delta = 117.8$ to 136.9 ppm) and do so the quaternary carbon atoms at $\delta = 114.7$ to 131.4 ppm. Out of this absorption range are only the carbons bound directly to oxygen ($\delta = 155.0$ and 157.9 ppm, respectively), and the carbonyl carbon itself ($\delta = 178.5$ ppm). In contrast, a similar general conclusion cannot be drawn from the analysis of the corresponding ^{1}H NMR spectrum of **11**. The aromatic protons

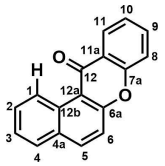

Figure 3. 12H-benzo[*a*]xanthen-12-one **11**

resonate in a completely normal way ($\delta = 7.47$ to 8.41 ppm) [with expected H,H-coupling values ($J_{ortho} = 7.5$ to 8.5 Hz, J_{meta} and $J_{para} < 1.5$ Hz)] except for H-1 ($\delta = 10.06$ ppm). This proton chemical shift of H-1 is widely outside of the resonance range of aromatic protons; usually only aldehyde protons can be expected so far low-field shifted. Therefore, the structure elucidation of **11** was far from ordinary. Finally, the DFT/GIAO calculation of this shift values ($\delta_{calc} = 10.9$ ppm) and reference 25 cleared up the present structure.

There are two reasonable but controversial reasons for this low-field position of H-1 in 12*H*-benzo[*a*]xanthen-12-one **11** out of the resonance range for aromatic protons:

(i) The combined ring current effect of the C-7a to 11a phenyl residue and the anisotropy effect of the carbonyl moiety.
(ii) *Steric compression* within the heavily hindered H(1)-C(1)-C(12b)-C(12a)-C(12)=O structural fragment. In this latter case, consequences on both the involved bond lengths and bond angles can be expected.

For this reason, the structure, the NMR chemical shifts (*vide supra*), and the spatial magnetic properties of 12*H*-benzo[*a*]xanthen-12-one **11** have been calculated (*cf.* Figure 4). We

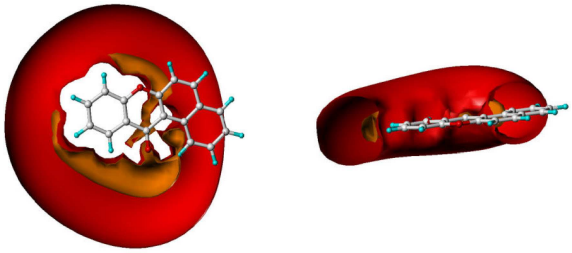

Figure 4. Visualization[26–28] of the in-plane spatial magnetic properties (TS NMRS) of 12*H*-benzo[*a*]xanthen-12-one (**11**) by the ICSS of −0.5 ppm (orange) and −0.1 ppm (red) *deshielding*.

employed our through-space NMR shielding concept (TS NMRS)[26–28] to qualify and quantify the spatial magnetic properties (actually, the familiar concept of anisotropy/ring current effect in ^{1}H NMR spectroscopy) of the studied conjugated species. Along this concept,[26–28] the TS NMRS are calculated as NICS values[29–30] for a grid of ghost atoms surrounding the molecules in order to locate diatropic and paratropic regions around the molecules. The TS NMRS values are visualized as iso-chemical-shielding surfaces (ICSS) of resulting NICS and were already employed to visualize and quantify the anisotropic effects of functional groups and the ring current effect of aromatic species and, hereby, present

(anti)aromaticity.[26–28] Specifications normally employed from magnetic point of view to quantify, *e.g.*, (anti)aromaticity, are theoretical non-measurable items:[31] single NICS values or components of the latter, or traces of NICS or components of the latter starting from the centre of the (anti)aromatic compound up to 10 Å outwards. Experimental $\Delta\delta$/ppm in proton NMR spectra, in turn, are the molecular response property of our TS NMRS values.[32–34] For this latter reason, the spatial magnetic properties (TS NMRS values) of 12*H*-benzo[*a*]xanthen-12-one **11** (and, *vide infra*, of the preferred conformers/diastereomers of the new *O,N*- and *N,N*-heterocycles) have been calculated and examined with respect to (i) the combined ring current effect of the C-7a to 11a phenyl residues and the anisotropy effect of the carbonyl moiety on the chemical shift of H-1 in **11** (*cf.* Figure 4). Proton H-1 is positioned within the deshielding belt [(ICSS) of −0.5 ppm (orange) and −0.1 ppm (red) deshielding] of this completely planar molecule; the exact value is −0.51 ppm deshielding.

Thus, the combined ring current effect of the C-7a to C-11a phenyl residue together with the anisotropy effect of the carbonyl moiety deshields the H-1 proton by about 0.5 ppm only. It remains a deshielding effect at least of *ca.* 1.5 ppm which must come from other resources, and this can be only (ii) *steric compression* within the heavily hindered H(1)-C(1)-C(12b)-C(12a)-C(12)=O structural fragment. From NMR spectra we have no direct access but the calculation of the structure of **11** indicates the corresponding consequences on both involved bond lengths and bond angles in **11**. The C(1)-H(1) bond length is shortened (normally 1.085 to 1.082 Å) and bond angles $<$C(12a,C(12b),C(1)=123.3°, $<$C(12),C(12a),C(12b)=123.6° and $<$O,C(12),C(12a)=124.7° are widened and document hereby, the steric hindrance in the studied H(1)-C(1)-C(12b)-C(12a)-C(12)=O structural fragment. Because ring current/anisotropy effects on H-1 is quantified to *ca.* −0.5 ppm deshielding for the present steric compression effect on $\delta(^1H)$/ppm at least *ca.* 1.5 ppm deshielding can be concluded. It is no surprise that for *steric compression* in **11** the value obtained was about the same as that in 11-ethynylphenanthrene.[35] The 11-ethynylphenanthrene molecule was employed to quantify the anisotropic effect of the –C≡C– triple bond, which should be −1.57 ppm deshielding around the triple bond. However, when employing our TS NMRS approach[26–28] we found that this effect is rather pretty showing only −0.06 ppm deshielding. The difference to −1.57 ppm deshielding results from *steric compression* within the 11-ethynylphenanthrene molecule.

2.4. Spatial Magnetic Properties (TS NMRS) of Preferred Regioisomers/diastereomers of the New *O,N*- and *N,N*-Heterocycles

The result of the NMR spectroscopic stereochemistry analysis of the reaction products of the studied [4+2] cycloaddition of the highly functionalized aminonaphthol derivatives (**4**, **19**, and **25**, respectively) *via* the *o*-QM intermediates (**5**, **20**, and **27**, respectively) proved to be unequivocal. Namely, in each case, when reacting various representative cyclic imines (**6**, **12**, and **15**, respectively) with **4** and **9**, the formation of one single product could be reported, which was unequivocally assigned to be the *trans* diastereomer for **8a**, **14a**, **17a** and **22a**. Furthermore, in the case of heterocycles formed starting from **25**, the relative *cis* configurations (**28b**, **30b** and **32b**) were assumed. As examples, both *O,N*-heterocycles **14a** and **17a** and *N,N*-heterocycles **30b** and **32b** were studied by our TS NMRS approach[26–28] (i) to prove the assigned diastereomers (*vide supra*) from the spatial magnetic point of view, and (ii) to find a simple NMR spectroscopic tool to readily differentiate the diastereomers.

In Figure 5, TS NMRSs of the preferred *trans* diastereomer **17a** are visualized by ICSS of 1 ppm (greenblue) and 0.5 ppm

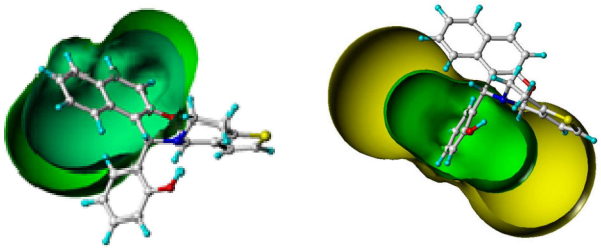

Figure 5. Visualization[26–28] of the spatial magnetic properties (TS NMRS) of both the naphthyl moiety (left) and of the phenol moiety of polyheterocycle **17a** by different ICSS of 1 ppm (greenblue), 0.5 ppm (green) and 0.1 ppm (yellow) *shielding*.

(green) *shielding* (for the ring current effect of the naphthyl moiety) and by ICSS of 0.5 ppm (green) and 0.1 ppm (yellow) *shielding* (for the ring current effect of the phenol moiety). In Figure 6, the corresponding TS NMRSs of the preferred *cis* diastereomer **32b** are visualized. In this case, because of additional influence, TS NMRS of the phenyl moiety are visualized by ICSS of −0.1 ppm (red) *deshielding*. Identical TS NMRS visualizations were obtained for **14a** and **30b** (*cf.* Table 4).

In **17a**, the naphthyl ring current effect on the phenoxy protons H-4′/5′ is *shielding* and it is extraordinarily large on the adjacent proton H-5′. The corresponding naphthyl protons H-1/2 are less affected (0.28 and 0.12 ppm *shielding*). The reversed effect is observed on the chemical shifts of the corresponding *trans* diastereomer protons: *shielding* on the protons of the phenyl moiety (H-3/4). The naphthoxy protons are less effected

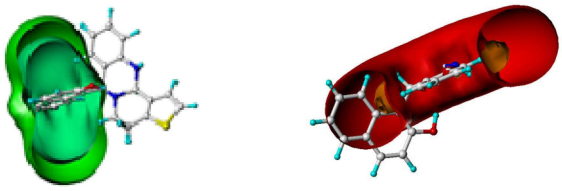

Figure 6. Visualization[26–28] of the spatial magnetic properties (TS NMRS) of both the naphthyl moiety (left) and of the phenol moiety of polyheterocycle **32b** by different ICSS of 1 ppm (greenblue) and 0.5 ppm (green) *shielding*, and −0.1 ppm (red) *deshielding*.

Table 4. Ring current effects of the phenyl/naphthyl moieties on protons H-1/2 and H-4′/5′ in **17 a**, and of the naphthyl/phenyl moieties on H-3/4 and H-7′/8′ in **32 b** as compared with the chemical shifts δ/ppm of the corresponding protons (in brackets).

Compd.	Ring current effects Δδ/ppm on				Ring current effects Δδ/ppm on			
	H-5′	H-4′	H-1	H-2	H-4	H-3	H-8′	H-7′
14 a	1.33 (6.51)	0.35 (6.65)	0.28 (7.41)	0.12 (7.37)				
17 a	1.34 (6.38)	0.35 (6.55)	0.28 (7.42)	0.12 (7.33)				
30 b					0.98 (6.54)	0.37 (6.57)	-0.24 (8.16)	-0.08 (7.57)
32 b					1.00 (6.45)	0.37 (6.48)	-0.23 (8.07)	-0.08 (7.48)

and it is even *deshielding* (−0.24 to −0.08 ppm). Identical results have been obtained for **14 a** and **30 b**, respectively (*cf.* Table 4).

The differences in the ring current effects [as calculated from TS NMRS values (*cf.* Table 4)], as being active in the diastereomers, are reproduced by the chemical shifts in the compounds studied. This is in no case remarkable. The experimental proton chemical shift δ(^{1}H)/ppm is the molecular response property of the spatial magnetic properties TS NMRS (*e.g.*, the anisotropy/ring current effect).[33–34] Both the chemical shift difference between the phenyl protons in the *cis* (**17 a**) and the *trans* diastereomer (**32 b**) [Δδ(H-5′-H-4) = 0.07 ppm, Δδ(H-4′-H-3 = −0.07 ppm] and the calculated ring current effects [Δδ(H-5′-H-4) = -0.34 ppm, Δδ(H-4′-H-3 = + 0.02 ppm] are comparable. In turn, the corresponding differences in Δδ(^{1}H)/ppm of the naphthyl protons are fairly different [Δδ(H-1-H-8′) = 0.65 ppm, Δδ(H-2-H-7′) = 0.15 ppm] in complete agreement with the calculated ring current effects [Δδ(H-1-H-8′) = 0.52 ppm, Δδ(H-2-H-7′) = 0.20 ppm]. Thus, the proton chemical shifts of the naphthyl protons can readily serve as simple indication of the present diastereomerism: H-7′ and H-8′ in the *cis* diastereomer are low field shifted with respect to H-1 and H-2 in the *trans* analogue. Thanks to TS NMRS (the ring current effects), the *cis*/*trans* diastereomers of the new *O*,*N*- and *N*,*N*-heterocycles can be simply differentiated.

3. Conclusions

Starting from salicylaldehyde and 2-naphthol or 6-hydroxyquinoline in the presence of morpholine, functionalized Mannich bases could be synthesized that served two different types of *o*-QM intermediates. While the relative stability of the formed *o*-QM intermediates was postulated to influence the formation of the products in the subsequent [4 + 2] cycloaddition, the highly functionalized aminodioles were reacted under heating with different cyclic imines such us 3,4-dihydroisoquinoline, 6,7-dihydrothieno[3,2-*c*]pyridine, and 3,4-dihydro-β-carboline. The latter reactions were found to be diastereo- and regioselective leading to *trans* naphthoxazine. Its structure was proved by DFT computed structures in comparison with the experimental ^{1}H/^{13}C-NMR spectra, and a detailed analysis of the spatial magnetic properties of the preferred diastereomers.

Mannich base **25** was synthesized as a unique substrate that was formed after thermal elimination *o*-QM and *aza*-*o*-QM. The functionalized diaminonaphthol was tested in [4 + 2] cycloaddition with cyclic imines **6**, **12**, and **15**. The regio- and diastereoselectivity of the reactions were proved by the same computational and ^{1}H/^{13}C NMR analysis; *cis*-quinazolines were isolated as single products.

The relative stability of *o*-QMs/*aza*-*o*-QM was examined by calculating their relative energies. The obtained results (**5 b** is more stable than **5 a**) supported completely the experimental findings, that naphthoxazines are formed during the cycloaddition reactions when aminodiole **4** was the starting compound. When diaminonaphthol **25** was applied as precursor, the regioselectivity of the reaction was found to be driven by the higher nucleophilicity of the amino group compared with the hydroxyl group.

During the synthesis and/or transformation of the functionalized aminonaphthols, unexpected heterocycles were achieved. Their formations were explained by the aim of the formed *o*-QMs and/or *aza*-*o*-QM and can be recommended as useful synthetic methods for benzo[*a*]xanthen-12-ones and benz[*a*]acridines, respectively.

Along the reaction of the *o*-QM intermediates **5 a,b** with dienophile 3,4-dihydro-β-carboline at higher temperatures (*e.g.*, 100 °C), 12*H*-benzo[*a*]xanthen-12-one **11** could be isolated as side product. The extreme low-field position of proton H-1 [δ(^{1}H) = 9.97 ppm] in **11** proved to be unusual and could be verified and quantified to be a combination of the paramagnetic ring current effect of the aromatic residues (together with the anisotropy effect of the carbonyl group, respectively) and steric compression within the heavily hindered H(1)-C(1)-C(12b)-H(12a)-C(12) = O structural fragment.

Experimental Section

Melting points were determined on a Hinotek X-4 melting point apparatus. Elemental analyses were performed with a Perkin-Elmer 2400 CHNS elemental analyser. Merck Kieselgel 60F_{254} plates were used for TLC. The microwave reactions were performed with a CEM Discover SP microwave reactor.

The used starting cyclic imines 4,9-dihydro-β-carboline[15] (**6**), 3,4-dihydroisoquinoline[21] (**12**), and 6,7-dihydrothieno[3,2-*c*]pyridine[22] (**15**) were synthesized according to the process known from the literature.

Quantum chemical calculations were performed using the Gaussian 09 program package[36] and carried out on LINUX clusters. The various different conformations and configurations of the studied compounds were optimized.[36] The B3LYP density functional method was selected for all calculations. The method is based on Becke's three-parameter hybrid functionals[37] and the correlation functional of Lee, Yang and Parr.[38] All optimizations were carried out without any restriction at this B3LYP/6-311G(d,p) level of theory.[39–40] NICS values[41] were computed using the gauge-including atomic orbital (GIAO) method[42–43] at the B3LYP/6-311G (d,p) theory level. Visualization was carried out with the modelling software SYBYL-X.[44]

The ^{1}H and ^{13}C NMR spectra were recorded in CD_2Cl_2 or [D_6]DMSO solution in 5 mm tubes at room temperature, on a Bruker Avance III

spectrometer at 600.13 (^{1}H) and 150.61 (^{13}C) MHz, with the deuterium signal of the solvent as the lock and TMS as internal standard. All spectra (^{1}H, ^{13}C, gs-H, H-COSY, edited HSQC, gs-HMBC and NOESY) were acquired and processed with the standard BRUKER software.

1-[(2-Hydroxyphenyl)-morpholin-4-yl-methyl]-2-naphthol (4)

2-Naphthol (2.0 g, 13.88 mmol), salicylic aldehyde (1.7 g, 13.90 mmol) and morpholine (1.21 g, 13.90 mmol) were stirred and heated at 80 °C under neat conditions for 5 h. Dichloromethane (100 ml) and water (100 ml) were added to the mixture that was then extracted with 2% hydrochloric acid. After separation of the fractions, the aqueous phase was alkalized with Na_2CO_3 and extracted with dichloromethane (2×70 ml). The organic fractions were collected, dried with anhydrous Na_2SO_4, filtered and then the solvent was removed under reduced pressure. The residue was crystallised with *n*-hexane (15 mL) and recrystallized from *i*Pr_2O (10 mL) R_f = 0.38 (*n*-hexane/ EtOAc, 2:1); 2.89 g (62%).

Beige crystals; m.p. 107–109 °C; ^{1}H NMR (CD_2Cl_2): δ = 2.57 (m, 1H, H-2″), 3.09 (m, 1H, H-2″), 3.62 (m, 1H, H-3″), 3.84 (m, 1H, H-3″), 5.84 (br s, 1H, H-8b), 6.80 (t, 7.7 Hz, 1H, H-5′), 6.82 (d, 8.1 Hz, 1H, H-3′), 7.10 (t, 7.8 Hz, 1H, H-4′), 7.13 (d, 8.9 Hz, 1H, H-3), 7.23 (t, 7.6 Hz, 1H, H-6), 7.35 (t, 7.9 Hz, 1H, H-7), 7.44 (dd, 7.8, 1.6 Hz, 1H, H-6′), 7.69 (d, 9.0 Hz, 1H, H-4), 7.71 (d, 8.7 Hz, 1H, H-5), 7.92 (d, 8.5 Hz, 1H, H-8), 13.50 (br s, 1H, 2-OH);^{13}C NMR (CD_2Cl_2): δ = 54.0 (br, C-2″), 62.8 (br, C-8b), 66.9 (C-3″),115.7 (2 C, br, C-1, C-3′), 119.9 (C-3), 121.6 (br, C-5′), 121.7 (C-8), 122.9 (C-6), 125.2 (br, C-1′), 126.8 (C-7), 128.9 (C-5), 129.0 (C-4a), 129.5 (C-4′), 129.6 (C-4), 130.5 (br, C-6′), 133.1 (C-8a), 154.0 (C-2′), 155.8 (C-2); elemental analysis calcd (%) for $C_{21}H_{21}NO_3$ (335.40) : C 75.20, H 6.31, N 4.18; found: C 75.16, H 6.34, N 4.13.

General Procedure for the Synthesis of Naphthoxazines (8 a, 14 a, and 17 a)

A mixture of the appropriate aminonaphthol **4** (40 mg 0.12 mmol), 4,5-dihydro-3*H*-benz[*c*]azepine **12** (26 mg, 0.18 mmol), 6,7- dihydrothieno[3,2-*c*]pyridine **15** (24 mg, 0.18 mmol), 3,4-dihydro-β-carboline **6** (30 mg, 0.18 mmol) in 1,4-dioxane (5 mL) was placed in a 10 mL pressurized reaction vial and heated in a CEM SP microwave reactor under the conditions given in Table 1. The solvent was removed *in vacuo,* and the residue was isolated by crystallization with MeOH (5 mL).

7a*R**,16*S**-17-(2-Hydroxyphenyl)-naphth[1,2-*e*]oxazino-[2,3-*a*]-β-carboline (8 a)

Recrystallized from *i*Pr_2O (5 mL); R_f = 0.38 (*n*-hexane/ EtOAc, 2:1); 44 mg (89%). Light brown crystals; m.p. 216–217 °C; ^{1}H NMR (CD_2Cl_2): δ = 2.97 (dd, *J* = 15.8, 3.5 Hz, 1H, H-13), 3.19 (ddd, *J* = 15.6, 12.1, 5.7 Hz, 1H, H-13), 3.35 (m, 2H, H-14), 5.84 (s, 1H, H-16), 5.99 (s, 1H, H-7a), 6.48 (d, *J* = 7.5 Hz, 1H, H-5′), 6.65 (t, *J* = 7.3 Hz, 1H, H-4′), 6.90 (d, *J* = 7.9 Hz, 1H H-2′), 7.08 (d, *J* = 8.9 Hz, 1H, H-6), 7.14 (t, *J* = 7.5 Hz, 1H, H-11), 7.18 (t, *J* = 7.2 Hz, 1H, H-3′), 7.23 (t, *J* = 7.6 Hz, 1H, H-10), 7.39 (m, 2H, H-3, H-9), 7.44 (t, *J* = 7.5 Hz, 1H, H-2), 7.54 (d, *J* = 8.3 Hz, 1H, H-1), 7.57 (m, 1H, H-12), 7.81 (d, *J* = 8.9 Hz, 1H, H-5), 7.85 (d, *J* = 7.9 Hz, 1H, H-4), 8.23 (br s, 1H, H-8), 9.52 (br s, 1H, H-1′);^{13}C (CD_2Cl_2): δ = 22.3(C-13), 45.3(C-14), 60.4(C-16), 77.3(C-7a), 109.4(C-16a), 110.8(C-12b), 111.7(C-9), 117.5(C-2′), 118.6(C-6), 119.3(C-12), 119.9(C-4′), 120.1(C-11), 122.5(C-1), 123.3(C-10), 124.0(C-3), 125.5(C-5a′), 126.2(C-12a), 127.3(C-2), 128.9(C-4),129.2(C-4a), 129.7(C-3′), 129.8(C-7b), 130.1(C-5), 130.7(C-5′), 132.8(C-16b), 150.8(C-6a), 156.9(C-1′); elemental analysis calcd (%) for $C_{28}H_{22}N_2O_2$ (418.50): C 80.36, H 5.30, N 6.69; found: C 80.41, H 5.27, N 6.74.

7a*R**,15*S**-15-(2-Hydroxyphenyl)-naphth[1,2-*e*]oxazino[2,3-*a*]-isoquinoline (14 a)

Recrystallized from *i*Pr_2O (6 mL); R_f = 0.38 (*n*-hexane/ EtOAc, 2:1); 40 mg (87%). White crystals; m.p. 206–207 °C; ^{1}H NMR (CD_2Cl_2): δ = 2.96 (m, 1H, H-12), 3.17 (m, 1H, H-13), 3.31 (m, 2H, H-12, H-13), 5.74 (s, 1H, H-15), 5.80 (s, 1H, H-7a), 6.51 (d, *J* = 7.6 Hz, 1H, H-5′), 6.65 (t, *J* = 7.4 Hz, 1H, H-4′), 6.89 (t, *J* = 8.0 Hz, 1H, H-2′), 7.08 (d, *J* = 8.9 Hz, 1H, H-6), 7.17 (t, *J* = 7.3 Hz, 1H, H-3′), 7.25 and 7.37 (2xm, 2x2H, H-8, H-9, H-10, H-11), 7.37 (m, 1H, H-3), 7.41 (t, *J* = 7.1 Hz, 1H, H-2), 7.50 (d, *J* = 8.3 Hz, 1H, H-1), 7.80 (d, *J* = 8.9 Hz, 1H, H-5), 7.83 (d, *J* = 7.9 Hz, 1H, H-4), 9.56 (br s, 1H, H-1′);^{13}C NMR (CD_2Cl_2): δ = 29.3(C-12), 43.9(C-13), 60.8(C-15), 81.5(C-7a), 109.1(C-15a), 117.4(C-2′), 118.8(C-6), 119.9(C-4′), 122.7(C-1), 123.9(C-3), 125.7(C-5a′), 126.6(C-10 or C-9), 127.2(C-2), 128.8(C-4), 129.1(C-8), 129.1(C-11), 129.2(C-4a), 129.5(C-9 or C-10), 129.6(C-3′), 130.1(C-5), 130.8(C-5′), 132.5(C-7b), 132.9(C-15b), 134.4(C-11a), 151.2(C-6a), 156.8(C-1′), elemental analysis calcd (%) for $C_{26}H_{21}NO_2$ (379.46):C 82.30, H 5.58, N 3.69; found: C 82.26, H 5.60, N 3.74.

7a*R**,14*S**-14-(2-Hydroxyphenyl)-naphth[1,2-*e*]oxazino[2,3-*a*]-thieno[3,2-*c*]pyridine (17 a)

Recrystallized from *i*Pr_2O (5 mL); R_f = 0.38 (*n*-hexane/ EtOAc, 2:1); 43 mg (92%). Light brown crystals; m.p. 186–187 °C; ^{1}H NMR (CD_2Cl_2): δ = 2.93 (m, 1H, H-11), 3.20 (m, 3H, H-11, H12), 5.69 (s, 1H, H-14), 5.74 (s, 1H, H-7a), 6.38 (d, *J* = 7.6 Hz, 1H, H-5′), 6.55 (t, *J* = 7.4 Hz, 1H, H-4′), 6.81 (t, *J* = 7.9 Hz, 1H, H-2′), 6.89 (d, *J* = 5.1 Hz, 1H, H-8), 7.00 (d, *J* = 8.9 Hz, 1H, H-6), 7.09 (t, *J* = 7.6 Hz, 1H, H-3′), 7.12 (d, *J* = 5.1 Hz, 1H; H-9), 7.28 (t, *J* = 7.3 Hz, 1H, H-3), 7.33 (t, *J* = 7.2 Hz, 1H, H-2), 7.42 (d, *J* = 8.2 Hz, 1H, H-1), 7.72 (d, *J* = 9.0 Hz, 1H, H-5), 7.75 (d, *J* = 7.9 Hz, 1H, H-4), 9.42 (br s, 1H, H-1′);^{13}C NMR (CD_2Cl_2): δ = 26.1(C-11), 44.6(C-12), 60.4(C-14), 78.3(C-7a), 109.1(C-14a), 117.5(C-2′); 118.7(C-6), 119.9(C-4′), 122.5(C-1), 123.9(C-3), 124.3(C-9), 125.6(C-5a′), 126.0(C-8), 127.3(C-2), 128.8(C-4), 129.2(C-4a), 129.7(C-3′), 130.1(C-5), 130.8(C-5′), 133.0(C-7b), 132.8(C-14b), 137.7(C-10a), 151.0(C-6a), 156.7(C-1′), elemental analysis calcd (%) for $C_{24}H_{19}NO_2S$ (385.48): C 74.78, H 4.94, N 3.63; found: C 74.82, H 4.92, N 3.69.

12*H*-Benzo[*a*]xanthen-12-one (11)

Aminonaphthol **4** (40 mg, 0.12 mmol), was heated with 2 equivalent of Et_3N (24.2 mg, 0.24 mmol) in 1,4-dioxane (5 mL) at 100 °C for 2 hour under microwave irradiation. The residue was purified by column chromatography (n-hexane: EtOAc, 3:1); 21 mg (71%); White solid; mp 144–146 °C (Lit.:[16] mp 145–146 °C).

5-[(2-Hydroxyphenyl)-morpholin-4-yl-methyl]-quinolin-6-ol (19)

6-Hydroxyquinoline (1.0 g, 6.88 mmol) was reacted with salicylic aldehyde (0,84 g. 6,88 mmol) in the presence of morpholine (0,60 g, 6.88 mmol). The reaction was stirred for 6 h at 80 °C, under neat conditions. The desired product was isolated by crystallization with *n*-hexane (10 ml) and recrystallized from *i*Pr_2O (8 mL). R_f = 0.38 (*n*-hexane/ EtOAc, 2:1); 1.64 g (71%). Brown crystals; m.p. 196–197 °C. ^{1}H NMR ([D_6]DMSO): δ = 2.44 (br s, 2H, H-2″), 3.67 (br s, 2H, H-3″), 5.71 (s, 1H, H-8b), 6.70 (t, 7.4 Hz, 1H, H-5′), 6.90 (d, 8.0 Hz, 1H, H-3′), 7.06 (t, 7.8 Hz, 1H, H-4′), 7.26 (d, 7.6 Hz, 1H, H-6′), 7.32 (d, 9.1 Hz, 1H, H-3), 7.38 (dd, 8.6, 4.1 Hz, 1H, H-7), 7.81 (d, 9.1 Hz, 1H, H-4), 8.26 (d, 8.4 Hz, 1H, H-8), 8.62 (d, 4.2 Hz, 1H, H-6), 10.20 (s, 1H, OH), 13.45 (s, 1H, OH); ^{13}C NMR ([D_6]DMSO): δ = 50.7 (br, C-2″), 61.7 (C-8b), 66.2 (C-3″),115.6 (C-3′), 115.9 (C-1), 120.0 (C-5′), 121.4 (C-7), 123.0 (C-3), 124.5 (C-1′), 127.4 (C-8a), 128.8 (C-6′), 129.2 (C-3′), 129.4 (C-8), 130.0 (C-4), 143.3 (C-4a), 146.7 (C-6), 154.7 (C-2′), 155.2 (C-2); elemental

analysis calcd (%) for $C_{20}H_{20}N_2O_3$ (336.39): C 71.41, H 5.99, N 8.33; found: C 71.48, H 5.96, N 8.37.

7a*R**,15*S**-15-(2-Hydroxyphenyl)-isoquinolino[1′,2′:2,3][1,3]-oxazin-o[5,6-f]quinolin (22 a)

Aminoquinolinol **19** (40 mg, 0.12 mmol), dihydroisoquinoline **12** (23 mg, 0.18 mmol) and 1,4-dioxane (5 mL) were placed in a 10 mL reaction vial and heated in a CEM microwave reactor under the conditions given in Table 1. The solvent was removed *in vacuo,* and the residue was isolated by crystallisation from MeOH (5 mL) and recrystallized from iPr_2O (10 mL). R_f = 0.38 (*n*-hexane/ EtOAc, 2:1); 34 mg (90%). Light brown crystals; m.p. 208–209 °C; ^{1}H NMR ([D_6] DMSO): δ = 2.84 (br d, *J* = 16.0 Hz, 1H, H-12), 3.05 (ddd, *J* = 16.7, 8.6, 8.6 Hz, 1H, H-12), 3.16 (m, 2H, H-13), 5.78 (s, 2H, H-7a, H-15), 6.61 (t, *J* = 7.0 Hz, 1H, H-4′), 6.66 (m, 1H, H-5′), 6.93 (d, *J* = 7.7 Hz, 1H, H-2′), 7.09 (t, *J* = 8.0 Hz, 1H, H-3′), 7.24 and 7.33 (2 x m, 2H and 1H, H-9, H-10, H-11), 7.34 (d, *J* = 9.2 Hz, 1H, H-6), 7.36 (dd, *J* = 8.5, 4.1 Hz, 1H, H-2), 7.41 (br d, *J* = 7.6 Hz, 1H, H-8), 7.63 (br d, *J* = 7.9 Hz, 1H, H-1), 7.89 (d, *J* = 9.2 Hz, 1H, H-5), 8.68 (dd, *J* = 4.2-1.6 Hz, 1H, H-3), 9.84 (br s, 1H, H-1′); ^{13}C NMR ([D_6]DMSO): δ = 28.5(C-12), 44.5(C-13), 55.9(C-15), 82.0(C-7a), 111.3(C-15a), 115.6(C-2′), 118.4(C-4′), 121.5(C-2 or C-6), 121.9(C-6 or C-2), 125.9(C-9), 126.5(C-15b), 128.5(C-10 or C-11), 128.7(C-3′), 128.8(C-5a′), 128.9(C-8), 128.9(C-11 or C-10), 129.5(C-5′), 129.8(C-5), 130.4(C-1), 132.2(C-7b), 134.9 (C-11a), 143.9(C-4a), 147.3(C-3), 151.8(C-6a), 155.1(C-1′); elemental analysis calcd (%) for $C_{25}H_{20}N_2O_2$ (380.45): C 78.93, H 5.30, N 7.36; found: C 78.89, H 5.36, N 7.71.

1-[(2-Nitrophenyl)-morpholin-4-yl-methyl]-naphthalen-2-ol (24)

50 ml round-bottom flask was charged with 2-naphthol (0.72 g, 5 mmol), morpholine (0.48 g, 5.5 mmol) and 2-nitrobenzaldehyde (0.79 g, 5.25 mmol). The mixture was stirred and heated under solvent-free conditions at 70 °C for 6 hours. The mixture was purified by column chromatography (*n*-hexane: EtOAc, 2:1); 1.31 g (72%). Yellow crystals; m.p. 148–149 °C; ^{1}H NMR (CD_2Cl_2): δ = 2.63 (dt, 11.8, 3.0 Hz, 1H, H-2″), 3.09 (d, 11.7 Hz, 1H, H-2″), 3.74 (dt, 11.7, 1.7 Hz, 1H, H-3″), 3.85 (t, 12.5 Hz, 1H, H-3″), 6.11 (s, 1H, H-8b), 7.13 (d, 8.9 Hz, 1H, H-3), 7.24 (ddd, 8.0, 6.9, 1.1 Hz, 1H, H-6), 7.36 (ddd, 8.6, 7.1, 1.5 Hz, 1H, H-7), 7.40 (dt, 7.8, 1.4 Hz, 1H, H-4′), 7.49 (dt, 7.7, 1.3 Hz, 1H, H-5′), 7.68 (d, 8.6 Hz, 1H, H-8), 7.71 (d, 8.1 Hz, 1H, H-5), 7.72 (d, 8.9 Hz, 1H, H-4), 7.85 (dd, 8.2, 1.3 Hz, 1H, H-3′), 7.88 (dd, 8.1, 1.5 Hz, 1H, H-6′), 13.46 (br s, 1H, 2-OH); ^{13}C NMR (CD_2Cl_2): δ = 54.0 (C-2″), 64.1 (C-8b), 66.9 (C-3″), 114.5 (C-1), 120.3 (C-3), 120.8 (C-8), 123.1 (C-6), 124.7 (C-3′), 127.3 (C-7), 129.0 (C-4a), 129.1 (C-5), 129.6 (C-4′), 130.6 (C-4), 131.5 (C-6′), 132.8 (C-8a), 133.0 (C-1′), 134.1 (C-5′), 150.6 (C-2′), 156.5 (C-2); elemental analysis calcd (%) for $C_{21}H_{20}N_2O_4$ (364.40): C 69.22, H 5.53, N 7.69; found: C 69.30, H 5.50, N 7.72.

1-[(2-Aminophenyl)-morpholin-4-yl-methyl]-naphthalen-2-ol (25)

(0.73 g, 2 mmol) of **24** was dissolved in 50 ml of EtOH and 0.2 g of 5% Pd/C catalyst was added. The mixture was hydrogenated at atmospheric pressure for 1 hour. After filtration of the catalyst, the solvent was removed and the residue was crystallized from Et_2O (30 mL) and recrystallized from iPr_2O (18 mL); 0.5 g (77%). Beige crystals; m.p. 133–134 °C; ^{1}H NMR (CD_2Cl_2): δ = 2.51 (ddd, 12.1, 9.3, 3.1 Hz, 1H, H-2″), 2.97 (m, 1H, H-2″), 3.76 (t, 9.2 Hz, 1H, H-3″), 3.82 (m, 1H, H-3″), 4.12 (br s, 2H, 2′-NH_2), 5.28 (s, 1H, H-8b), 6.66 (t, 7.5 Hz, 1H, H-5′), 6.71 (d, 7.9 Hz, 1H, H-3′), 7.03 (t, 7.6 Hz, 1H, H-4′), 7.10 (d, 8.9 Hz, 1H, H-3), 7.23 (t, 7.5 Hz, 1H, H-6), 7.33 (d, 7.7 Hz, 1H, H-6′), 7.36 (ddd, 8.5, 7.0, 1.4 Hz, 1H, H-7), 7.68 (d, 9.0 Hz, 1H, H-4), 7.71 (,d, 8.2 Hz, 1H, H-5), 7.76 (d, 8.6 Hz, 1H, H-8), 13.37 (br s, 1H, 2-OH); ^{13}C NMR (CD_2Cl_2): δ = 53.9 (br, C-2″), 67.0 (C-3″),114.7 (br, C-1), 117.1 (C-3′), 119.7 (br, C-5′), 120.0 (C-3), 121.8 (C-8), 122.9 (C-6), 123.0 (br, C-1′), 126.8 (C-7), 129.0 (C-5), 129.0 (C-4a), 129.3 (C-4′), 129.8 (C-4), 130.6 (br, C-6′), 133.0 (C-8a), 145.0 (C-2′), 155.7 (C-2), C-8b could not be detected (very broad line); elemental analysis calcd (%) for $C_{21}H_{22}N_2O_2$ (334.17): C 75.42, H 6.63, N 8.38; found: C 75.45, H 6.60, N 8.37.

Benz[*a*]acridine (26)

The synthetic protocol applied to achieve **25** was repeated, and the reaction was driven till the formation of **26** (5 hours). After removal of the catalyst, the filtrate was concentrated under reduced pressure and the crude reaction mixture was purified by column chromatography (*n*-hexane:EtOAc, 2:1) resulting in **26** (0.32 g, (69%); Beige crystals; m.p. 129–130 °C (Lit.:[24] mp 130–131 °C).

General Procedure for the Synthesis of Quinazolines (28 b, 30 b and 32 b)

A mixture of diaminonaphtol **25** (67 mg 0.2 mmol) and 3,4-dihydro-β-carboline **6** (50 mg, 0.3 mmol), or 3,4-dihydroisoquinoline **12** (39.4 mg, 0.3 mmol) or 6,7-dihydrothieno[3,2-*c*]pyridine **15** (41.2 mg, 0.3 mmol), in 1,4-dioxane (5 mL) was placed in a 10 mL pressurized reaction vial and heated in a CEM SP microwave reactor under the conditions given in Table 2. The solvent was removed under reduced pressure and the residue was isolated by crystallization from MeOH and recrystallized.

5S,13bS**-7-(2-Hydroxynaphth-1-yl)-[2,3-*a*]-β-carbolino[2,1-*b*]-quinazoline (28 b)

Recrystallized from iPr_2O (6 mL); R_f = 0.38 (*n*-hexane/EtOAc 2:1); 76 mg (91%). Beige crystals; m.p 182–183 °C; ^{1}H NMR ([D_6]DMSO): δ = 2.71 (m, 1H, H-8), 2.79 (m, 1H, H-8), 2.80 (m, 1H, H-7), 3.09 (m, 1H, H-7), 5.27 (br s, 1H, H-13b), 6.10 (s, 1H, H-5), 6.41 (d, *J* = 8.0 Hz 1H, H-4), 6.48 (m, 1H, H-14), 6.49 (m, 1H, H-3), 6.80 (d, *J* = 7.5 Hz, 1H, H-1), 7.01 (m, 2H, H-11, H-3′), 7.02 (m, 1H, H-2′), 7.14 (d, *J* = 8.4 Hz, 1H, H-9), 7.38 (t, *J* = 7.4 Hz, 1H, H-6′), 7.45 (m, 2H, H-10, H-12), 7.59 (t, *J* = 7.6 Hz, 1H, H-7′), 7.79 (d, *J* = 8.8 Hz, 1H, H-4′), 7.89 (d, *J* = 7.8 Hz, 1H, H-5′), 8.29 (d, *J* = 8.6 Hz, 1H, H-8′), 11.09 (s, 1H, H-13), 11.82 (br s, 1H, H-2′); ^{13}C ([D_6]DMSO): δ = 21.0(C-8), 47.7(C-7), 61.0(C-5), 68.2(C-13b), 108.2(C-8b), 111.5(C-12), 116.5(C-1), 117.8(C-1′), 118.2(C-10), 119.0(C-3 or C3′), 119.4(C-3′ or C-3), 119.4(C-11), 121.5(C-9), 121.8(C-8′), 122.6(C-6′), 123.8(C-4a), 125.8(C-8a), 127.1(C-7′ or C-2), 127.2(C-2 or C-7), 127.3(C-4), 128.0(C-4a′), 128.7(C-5′), 129.3(C-4′), 131.5(C-13a), 134.1(C-8a′), 136.3(C-12a), 143.0(C-14a), 155.5(C-2′), elemental analysis calcd (%) for $C_{26}H_{22}N_3O$ (417.51): C 80.55, H 5.55, N 10.06; Found: C 80.48, H 5.57, N 10.04.

5S,12bS**-7-(2-Hydroxynaphth-1-yl)-[2,3-*a*]isoquinolino-[2,1-*b*]-quinazoline (30 b)

Recrystallized from iPr_2O (7 mL); R_f = 0.38 (*n*-hexane/EtOAc 2:1); 67 mg (89%). White crystals; m.p. 191–192 °C; ^{1}H NMR (CD_2Cl_2): δ = 2.61 (ψt, *J* = 13.8 Hz, 1H, H-7), 2.71 (d, *J* = 14.7 Hz, 1H, H-8), 3.19 (m, 2H, H-7, H-8), 4.36 (d, *J* = 5.6 Hz, 1H, H-13), 5.14 (d, *J* = 5.9 Hz, 1H, H-12b), 5.83 (s, 1H, H-5), 6.54 (m, 1H, H-4), 6.57 (m, 1H, H-3), 6.87 (d, *J* = 7.9 Hz, 1H, H-1), 7.06 (m, 2H, H-2, H-3′), 7.19 (d, *J* = 7.2 Hz, 1H, H-9), 7.31 (m, 1H, H-10), 7.35 (m, 1H, H-11), 7.38 (m, 1H, H-6′), 7.57 (t, *J* = 7.5 Hz, 1H, H-7′), 7.65 (d, *J* = 7.4 Hz, 1H, H-12), 7.76 (d, *J* = 8.7 Hz, 1H, H-4′), 7.85 (d, *J* = 8.0 Hz, 1H, H-5′), 8.16 (d, *J* = 8.5 Hz, 1H, H-8′), 11.38 (br s, 1H, H-2′);^{13}C (CD_2Cl_2): δ = 29.3(C-8), 47.3(C-7), 63.0(C-5),

72.7(C-12b), 117.5(C-1′), 118.0(C-1), 120.0(C-3′), 120.6(C-3), 121.7(C-8′), 122.9(C-6′), 124.8(C-4a), 125.4(C-12), 127.0(C-11), 127.3(C-7′), 127.9(C-2), 128.2(C-10), 128.2 (C-4), 128.8(C-4a′), 129.1(C-9), 129.1(C-5′), 129.8 (C-4′), 134.6(C-8a′), 135.0(C-12a), 135.4(C-8a), 142.5(C-13a), 155.5(C-2′); elemental analysis calcd (%) for $C_{26}H_{22}N_2O$ (378.48): C 82.51, H 5.86, N 7.40; found: C 82.67, H 5.88, N 7.38.

5S,11bS**-7-(2-Hydroxynaphth-1-yl)-thieno[3,2-c]pyrido-[2,1-*b*]quinazoline (32 b)

Recrystallized from iPr_2O (6 mL); $R_f = 0.38$ (*n*-hexane/EtOAc 2:1); 71 mg (92%). White crystals; m.p. 198–199 °C; ^1H NMR (CD_2Cl_2): δ 2.62 (td, $J = 11.8$, 3.7 Hz, 1H, H-7), 2.70 (br d, $J = 16.4$ Hz, 1H, H-8), 3.02 (br t, $J = 14.0$ Hz, 1H, H-8), 3.16 (ddd, $J = 11.8$, 5.3, 1.4 Hz, 1H, H-7), 4.24 (d, $J = 5.8$ Hz, 1H, H-12), 4.93 (d, $J = 5.8$ Hz 1H, H-11b), 5.75 (s, 1H, H-5), 6.45 (m, 1H, H-4), 6.48 (ddd, $J = 7.9$, 6.9, 1.1 Hz, 1H, H-3), 6.74 (dd, $J = 8.0$, 0.8 Hz, 1H, H-1), 6.95 (d, $J = 6.95$ Hz, 1H, H-3′), 6.97 (br t, $J = 7.5$ Hz, 1H, H-2), 7.08 (d, $J = 5.2$ Hz, 1H, H-11), 7.19 (dd, $J = 5.2$, 0.6 Hz, 1H, H-10), 7.29 (ddd, $J = 8.5$, 6.9, 1.5 Hz, 1H, H-6′), 7.48 (ddd, $J = 8.5$, 6.9, 1.5 Hz, 1H, H-7′), 7.66 (d, $J = 8.8$ Hz, 1H, H-4′), 7.75 (d, $J = 8.0$ Hz, 1H, 5′), 8.07 (d, $J = 8.6$ Hz, 1H, H-8′), 11.18 (br s, 1H, H-2′); ^{13}C (CD_2Cl_2): δ = 25.5(C-8), 48.1(C-7), 62.1(C-5), 71.3(C-11b), 117.7(C-1′), 117.8(C-1), 120.0(C-3′), 120.7(C-3), 121.7(C-8′), 123.0(C-6′), 123.9(C-11), 124.7(C-10), 124.8(C-4a), 127.3(C-7′), 127.9(C-2), 128.2(C-4), 128.9(C-4a′), 129.2(C-5′), 129.8(C-4′), 134.3(C-8a′), 134.5(C-11a), 136.7(C-8a), 142.2(C-12a), 155.5(C-2′); elemental analysis calcd (%) for $C_{24}H_{20}N_2OS$ (384.50): C 74.97, H 5.24, N 7.29; Found: C 74.95, H 5.26, N 7.34.

Acknowledgements

The authors thank the Ministry of National Economy, National Research Development and Innovation Office [GINOP-2.3.2-15-2016-00038], the EU-funded Hungarian Grant [EFOP-3.6.1-16-2016-00008], and the Ministry of Human Capacities, Hungary Grant, 20391-3/2018/FEKUSTRAT.

Conflict of Interest

The authors declare no conflict of interest.

Keywords: *ortho*-quinone methide (*o*-QMs) · modified Mannich reaction · cycloaddition · NMR spectroscopy · conformational analysis · DFT calculations

[1] S. K. Bur, S. F. Martin, *Tetrahedron* **2001**, *57*, 3221–3242.
[2] W. N. Speckamp, M. J. Moolenaar, *Tetrahedron* **2000**, *56*, 3817–3856.
[3] X. Lian, L. Lin, K. Fu, B. Ma, X. Liu, X. Feng, *Chem. Sci.* **2017**, *8*, 1238–1242.
[4] J. F. A. Filho, B. C. Lemos, A. S. de Souza, S. Pinheiro, S. J. Greco, *Tetrahedron* **2017**, *73*, 6977–7004.
[5] I. Szatmári, F. Fülöp, *Tetrahedron* **2013**, *69*, 1255–1278.
[6] B. Karmakar, J. Banerji, *Tetrahedron Lett.* **2011**, *52*, 4957–4960.
[7] P. Barta, I. Szatmári, F. Fülöp, M. Heydenreich, A. Koch, E. Kleinpeter, *Tetrahedron* **2016**, *72*, 2402–2410.
[8] P. Barta, F. Fülöp, I. Szatmári, *Beilstein J. Org. Chem.* **2018**, *14*, 560–575.
[9] V. A. Osyanin, D. V. Osipov, Y. N. Klimochkin, *Tetrahedron* **2012**, *68*, 5612–5618.
[10] J. D. Pettigrew, R. P. Freeman, P. D. Wilson, *Can. J. Chem.* **2004**, *82*, 1640–1648.
[11] H. H. Liao, A. Chatupheeraphat, C. C. Hsiao, I. Atodiresei, M. Rueping, *Angew. Chemie, Int. Ed.* **2015**, *54*, 15540–15544.
[12] I. Szatmári, F. Fülöp, *Tetrahedron Lett.* **2011**, *52*, 4440–4442.
[13] I. Szatmári, P. Barta, A. Csámpai, F. Fülöp, *Tetrahedron* **2017**, *73*, 4790–4804.
[14] V. A. Osyanin, E. A. Lvleva, Y. N. Klimochkin, *Chem. Heterocycl. Compd.* **2012**, *48*, 795–798.
[15] Z. Chen, G. Hu, D. Li, J. Chen, Y. Li, H. Zhou, Y. Xie, *Bioorg. Med. Chem.* **2009**, *17*, 2351–2359.
[16] J. Tang, S. Zhao, Y. Wei, Z. Quan, C. Huo, *Org. Biomol. Chem.* **2017**, *15*, 1589–1592.
[17] K. Okuma, A. Nojima, N. Matsunaga, K. Shioji, *Org. Lett.* **2009**, *11*, 169–171.
[18] J. Zhao, R. C. Larock, *Org. Lett.* **2005**, *7*, 4273–4275.
[19] J. Zhao, R. C. Larock, *J. Org. Chem.* **2007**, *72*, 583–588.
[20] S. Wang, K. Xie, Z. Tan, X. An, X. Zhou, C. C. Guo, Z. Peng , *Chem. Commun.* **2009**, *42*, 6469–6471.
[21] I. Szatmári, J. Sas, F. Fülöp, *Tetrahedron Lett.* **2013**, *54*, 5096–5071.
[22] W. Herz, L. Tsai, *J. Chem. Soc.* **1955**, 77, 3529–3533.
[23] O. Bilgic, D. W. Young, *J. Chem. Soc. Perkin Trans. 1* **1980**, *1*, 1233–1239.
[24] I. Szatmári, M. Heydenreich, A. Koch, F. Fülöp, E. Kleinpeter, *Tetrahedron* **2013**, *69*, 4755–7465.
[25] A. M. S. Silva, D. C. G. A. Pinto, H. R. Travares, J. A. S. Cavaleiro, M. L. Jimeno, J. Elguero, *Eur. J. Org. Chem.* **1998**, 2031–2039.
[26] S. Klod, E. Kleinpeter, *J. Chem. Soc. Perkin Trans. 2* **2001**, 1893–1898.
[27] E. Kleinpeter, S. Klod, A. Koch, *J. Mol. Struct. (THEOCHEM)* **2007**, *811*, 45-60 and references cited therein.
[28] Kleinpeter, *Annual Reports on NMR Spectroscopy (edited by Graham A. Webb), ELSEVIER, Vol. 82 (2014) - Chapter 3:* Quantification and Visualization of the Anisotropy Effect in NMR Spectroscopy by Through-Space NMR Shieldings.
[29] P. v. R. Schleyer, C. Maerker, A. Dransfield, H. Jiao, H. N. J. Van Eikema Hommes, *J. Am. Chem. Soc.* **1996**, *118*, 6317–6318.
[30] Z. Chen, C. S. Wannere, C. Corminboeuf, R. Puchta, P. v. R. Schleyer, *Chem. Rev.* **2005**, *105*, 3842–3888.
[31] A. Stanger, *Chem. Commun.* **2009**, 1939–1947.
[32] A. Lämmermann, H. Kühn, E. Kleinpeter, *Org. Biomol. Chem.* **2011**, *9*, 1098–1111.
[33] E. Kleinpeter, A. Koch, *J. Phys. Chem. A* **2012**, *116*, 5674–5680.
[34] E. Kleinpeter, A. Koch, *Phys. Chem. Chem. Phys.* **2012**, *14*, 8742–8746.
[35] E. Kleinpeter, S. Klod, *J. Am. Chem. Soc.* **2004**, *126*, 2231–2236.
[36] M. J. Frisch Gaussian 09, Revision A.02. Wallingford, CT: Gaussian, Inc. **2009**
[37] A. D. Becke *J. Chem. Phys.* **1993**, *98*, 5648–5652.
[38] C. Lee, W. Yang, R. G. Parr *Phys. Rev. B* **1988**, *37*, 785–789.
[39] W. J. Hehre L. Radom, P. von Rague Schleyer *J. Pople Ab Initio Molecular Orbital Theory*; Wiley: New York, NY, **1986**.
[40] A. D. Becke *J. Chem. Phys.* **1993**, *98*, 1372–1492.
[41] P. von Rague Schleyer, C. Maerker, A. Dransfeld, H. Jiao, N. J. R. van E. Hommes *J. Am. Chem. Soc.* **1996**, *118*, 6317–6318.
[42] R. Ditchfield *Mol. Phys.* **1974**, *27*, 789–807.
[43] G. W. Cheeseman, T. A. Trucks, M. J. Keith *J. Chem. Phys.* **1996**, *104*, 5497–5509.
[44] SYBYL-X 2.1.1. Tripos, 2013, 1699 South Hanley Road, St. Louis, MO 63144, USA.

Manuscript received: April 30, 2019
Revised manuscript received: June 7, 2019